Simultaneous Control of Velocity and Field Flux of DC Nonlinear Motors

Cuauhtémoc Guerrero, Víctor Santibañez, *Member IEEE*

***Abstract*—This paper presents a novel strategy that exploits the properties presented by the nonlinear model of direct current motors, to obtain simultaneously the required control voltages in the armature and in the field windings when velocity and magnetic flux are considered as reference inputs. In this scheme, it is considered that the current signals for both windings are available, as well as the signal of the angular position. So by means of a second order filter, the signal that takes the place of the angular velocity is obtained. By using the Lyapunov stability theory, stability of the closed loop system, global convergence of angular velocity and field flux is concluded, moreover all the states variables are bounded for all initial conditions. Experimental tests confirm the theoretical proposal; that is, global asymptotic tracking of the angular velocity and field flux is ensured. The equations of this proposal are physically implementable and due to the structure of the control scheme, the voltages of both windings can be tuned in such a way that less current dissipates, resulting in energy saving and having the same response of velocity.**

***Index Terms*—Field Flux, Nonlinear Model, Passivity, Second Order Filter, Stability Analysis.**

I. INTRODUCTION

THE Direct Current (DC) motors are still considered as the usual option, when a system is controlled for a wide range of velocities, because of its excellent operational properties and control characteristics. Effectively, the DC machine was widely used for a long time in adjustable velocity drives, but due to the strong development of power electronics technologies and control theory applied to AC machines, the DC machines are being relegated in certain areas, but in many traditional industries are still used [1].

In high-performance motion applications, such as in robotic manipulator position tracking, machine tool manufacturing, high-speed industrial automation, etc., there is the need for accurate, positioning and / or speed control. To achieve the latter, many systems continue to use DC motors to perform mechanical traction, so some inherent problems in these task still present challenges to solved when considering one or more control performance specifications (e.g., tracking trajectories of reference, rejection of disturbances, robustness, among others). The separately excited DC motor, in its model can have a linear structure if the field windings are excited the form constat, that is, have a constant magnetic flux in the field, so that the DC motor velocity control with this structure, theoretically, is a solved problem and there is a lot of information about linear control strategies in many textbooks (see e.g. [2, chap. 10]); However in high performance applications in which the control of position and/or velocity with high accurate is critical, the control still presents some challenges for implementation. It should be mentioned that in recent publications the classical PID control structure is applied by tuning the gains using optimization techniques, such as the works reported in [3], [4] and [5].

Traditionally, DC motors are coupled with power electronic converter and position (or velocity) measurement devices, so a large majority of works reported in over the last few years for velocity control of such motors, do it through the use of mathematical models with linear structures, but the design of the controllers is carried out applying nonlinear control techniques. These publications can be classified into two large groups. The first group takes into account the structure of the power converter in conjunction with the linear model of the motor as in [6] a control scheme design is shown, where simultaneously, the velocity of the DC motor and the duty ratio of the power devices to obtain a unity power factor of the three-phase power supply, while in [7] a controller based on the combination of passivity techniques and Differential Flatness property is presented as well as in [8] the velocity control is performed by optimizing the duty ratio and estimating the states by means of a generalized proportional-integral observer. On the other hand, DC-DC boost converters are considered as extra dynamics, e.g. in [9] designed a nonlinear PI velocity controller for providing the duty ratio input, and in [10] a scheme that controls the complete system by combining pulse frequency modulation, pulse width modulation and phase angle shift, is designed. The second group considers only the linear model of the motor, but uses nonlinear control techniques; for example, in [11], a PID controller with parallel and antiwindup structure (whose tuning of gains is analytical) and a passivity based controller are shown, both controllers consider only the position measurement; in [12] an observer-based velocity controller is designed using a triple-step nonlinear method; while [13] shows the topology of a fractional order controller performed by the inverse-follow-the-leader feedback applied to the linear model of the DC motor.

The work shown in this paper uses the mathematical model the separately excited DC motor with a structure that is nonlinear and applies techniques that take advantage of

Manuscript received Month xx, 2xxx; revised Month xx, xxxx; accepted Month x, xxxx. This work was supported in part by the Universidad Autónoma de la Ciudad de México and CONACYT Project 134534 and TecNM Projects.

C. Guerrero is with the Academic of Ingeniería en Sistemas Electrónicos Industriales, Universidad Autónoma de la Ciudad de México, Ciudad de México, 09790, Ciudad de México, México (corresponding author to provide phone: +52 5550581901, ext. 13163; e-mail: cuauhtmoc.guerrero@uacm.edu.mx).

V. Santibañez is with the Tecnológico Nacional de México/Instituto Tecnológico de la Laguna, Torreón, Coahuila, 27000, México (e-mail: vsantiba@itlaguna.edu.mx).

passivity properties inherent in such a nonlinear model, in order to design a control strategy. It is worth mentioning that there are publications where the nonlinear model of the DC motor is considered. A pioneering work is that of [14], where through differential-geometric methods (by means of an exact linearization) the velocity control is designed taking into account that state signals are available in the first instance having as input both voltages, in the field and armature windings, to perform the so-called armature control an later by keeping fixed the armature voltage to perform the field control. Other works use feedback linearization techniques, as in [15], considering the separately excited DC motor as a multiple input and multiple output nonlinear system, to operate in high speed ranges with field weakening. On the other hand, in [16] the authors use a passivity-based methodology to design control strategies for three configurations of the DC motor, considering the availability of full state signals, exact knowledge of the parameters of the machine, and unknown but constant load torque.

In the present work, a control strategy is proposed in which two variables are simultaneously considered as references: one is the reference of the angular velocity and the other one is the reference of the magnetic flux of the field windings. It is worth mentioning that in the design of the proposal, the availability of the angular position signal (not the angular velocity) is considered, integrals of the current errors have been incorporated in the structures of the control voltages (armature and field), whose use is mathematically justified in the stability analysis. The control scheme presented is a novel alternative for DC machines to be used in tasks with high-performance specifications and at the same time saving energy, especially when the motor is running at a constant velocity, the field flux reference can be varied to develop less power for both field and armature windings. Despite having a relatively complex structure compared to traditional control designs, this controller has the advantage that the equations that comprise it are physically implementable, as well ensures the tracking of the both time variant signals references (velocity and flux field) and ensures that the power demanded by machine is within the manufacturer's specifications; the fact of incorporating error integrals is to match with this very common practice in industrial applications.

In sum, in our proposal the contributions of the introduced control scheme are: a) global convergence of the velocity angular to track time variant profiles of velocity is ensured by means of the Lyapunov stability theory, b) furthermore the control scheme also simultaneously ensures the tracking of the field flux, which may results in energy saving for same response of velocity (see Fig. 4 shown later on, in Section IV) and c) the controller requires only the position signal, and the signals of currents for both windings (field and armature), that is the controller equations are physically implementable in an easy way.

II. Nonlinear mathematical model of the separately excited direct current motor.

There are three equations that describe the characteristics of a separately excited DC motor [14]. One is that related with the balance of voltages in the windings of the field, for analysis issues, it is assumed that there is no flux leakage in the air gap. For reasons inherent in the manufacturing materials of windings, it is considered that there is a linear function of the magnetization curve that relates, in the field windings [14], the field flux (linkage) ϕ_f versus the field current i_f as

$$\phi_f\left(i_f\right) = L_f i_f \tag{1}$$

where L_f is the inductance of the stator windings, therefore, by considering that (in these same windings) v_f denotes the voltage supplied to the terminals, while R_f denotes the resistance, and applying Kirchhoff's voltage law, it results

$$v_f = \frac{R_f}{L_f}\phi_f + \frac{d}{dt}\phi_f \tag{2}$$

The equation that is present in the rotor windings, is

$$v_a = R_a i_a + L_a \frac{d}{dt} i_a + K_\phi \phi_f \omega \tag{3}$$

where R_a and L_a are the resistance and inductance, respectively, that are present in the armature windings, K_ϕ is a proportionality constant, while i_a is the current that is produced in this winding when it is excited by a voltage v_a and ω denotes the rotor angular velocity.

For the mechanical part, it has an equation relating the rotating forces in the rotor shaft as

$$J\frac{d}{dt}\omega + B\omega = K_\phi \phi_f\, i_a - \tau_L \tag{4}$$

with the viscous friction constant and the moment of inertia denoted by B and J respectively, while τ_L is the load torque applied to the motor shaft.

Defining the state vector as $\mathbf{x} = \begin{bmatrix}\phi_f & i_a & \omega\end{bmatrix}^T \in \mathbb{R}^3$ and considering (2)-(4), the state equations can be written as

$$\boldsymbol{\mathcal{D}}\,\dot{\mathbf{x}} + \boldsymbol{\mathcal{R}}\,\mathbf{x} + \boldsymbol{\mathcal{C}}\left(\phi_f\right)\,\mathbf{x} = \mathbf{u} \tag{5}$$

where $\mathbf{u} = \begin{bmatrix}v_f & v_a & -\tau_L\end{bmatrix}^T \in \mathbb{R}^3$ is the input vector and

$$\boldsymbol{\mathcal{D}} = \begin{bmatrix}1 & 0 & 0\\ 0 & L_a & 0\\ 0 & 0 & J\end{bmatrix}, \qquad \boldsymbol{\mathcal{R}} = \begin{bmatrix}\frac{R_f}{L_f} & 0 & 0\\ 0 & R_a & 0\\ 0 & 0 & B\end{bmatrix},$$

$$\boldsymbol{\mathcal{C}}\left(\phi_f\right) = \begin{bmatrix}0 & 0 & 0\\ 0 & 0 & K_\phi\phi_f\\ 0 & -K_\phi\phi_f & 0\end{bmatrix} \tag{6}$$

with $\boldsymbol{\mathcal{D}} \in \mathbb{R}_+^{3x3}$ and $\boldsymbol{\mathcal{R}} \in \mathbb{R}_+^{3x3}$ are diagonal matrix and $\boldsymbol{\mathcal{C}}\left(x_1\right) \in \mathbb{R}^{3x3}$ is a skew-symmetric matrix.

Remark 1. For physical reasons, the motor parameters are all positive and with this the matrices $\boldsymbol{\mathcal{D}}$ y $\boldsymbol{\mathcal{R}}$ given in (6) are positive definite. Also, the matrix $\boldsymbol{\mathcal{C}}\left(\phi_f\right)$ is skew-symmetry; which leads to $\mathbf{x}^T\boldsymbol{\mathcal{C}}\left(\phi_f\right)\mathbf{x} = 0$. On the other hand, if a storage function is considered as $\mathcal{H}\left(\mathbf{x}\right) = \frac{1}{2}\mathbf{x}^T\boldsymbol{\mathcal{D}}\mathbf{x}$, the separately excited DC motor model (5) represents a passive mapping of inputs to states, as it is demonstrated in [16].

III. Main result.

A. Problem formulation.

Consider the nonlinear mathematical model of the separately excited DC motor in matrix form given by (5). Suppose that:

A.1 The measurement of the signals of the currents of the armature windings i_a and of the field windings i_f, as well as the angular position of the rotor θ are available.

A.2 All the parameters of the separate excitation direct current motor model are known.

This article has been accepted for publication in a future issue of this journal, but has not been fully edited. Content may change prior to final publication. Citation information: DOI 10.1109/TIE.2021.3068683, IEEE Transactions on Industrial Electronics

A.3 The desired angular velocity of the rotor ω_d is a bounded and twice differentiable function, where the first and second order time derivative have known bounds, such that $|\dot{\omega}_d| \leq k_{1\omega} < \infty, \ \ \forall t \in [0, \infty)$.

A.4 The desired flux of the field ϕ_{fd} is a strictly positive bounded differentiable function, with known bounds of it and, of its first-order time derivative, such that, $0 < k_{1\phi} \leq \phi_{fd} \leq \phi_{fd}^{max} < \infty$ and $\dot{\phi}_{fd} \leq \dot{\phi}_{fd}^{max} < \infty$.

A.5 The load torque τ_L is an unknown constant function.

The problem of control is: to find the field and armature voltages of the nonlinear DC motor, having the measurements of the angular position of the rotor available, as well as the currents of the armature and field windings, so that the closed loop system has a global asymptotic tracking, simultaneously, of the angular velocity and field flux, with all internal variables bounded.

B. Proposed controller

Let the control voltage for the armature windings be proposed as

$$v_a = L_a \frac{d}{dt} i_{ad} + R_a i_{ad} + K_\phi \phi_{fd} \omega_d + K_{pa} e_a + K_{ia} \xi_a \quad (7)$$

where i_{ad} is the desired current of the armature, ϕ_{fd} is the desired flux and ω_d is the desired velocity, while e_a and e_f denote the errors of the armature current and the field flux, defined ahead in (20) as well as the constants K_{pa} and K_{ia} are the proportional and integral gains, respectively.

The control voltage of the field windings is proposed as

$$v_f = \frac{d}{dt}\phi_{fd} + \frac{R_f}{L_f}\phi_{fd} - K_\phi \omega_d e_a + K_{pf}\, e_f + K_{if}\xi_f \quad (8)$$

with the constants K_{pf} and K_{if} being the proportional and integral gains, respectively. The third term on the right side of (8) is a voltage of mechanical origin that is obtained from the desired velocity, analogous to the last term on the right side is in (3), and is key to get passivity in the closed loop system by means of the skew-symmetry of the matrix $\boldsymbol{\mathcal{C}}$ in (23).

The last terms on the right side of (7) and (8) define variables of the integral terms of both currents errors, i.e.,

$$\xi_f = \int_0^t e_f dt \qquad \xi_a = \int_0^t e_a dt \quad (9)$$

The desired armature current is obtained by means of

$$i_{ad} = \frac{1}{K_\phi\, \phi_{fd}} \left(\hat{\tau}_L + J\dot{\omega}_d + B\omega_d - K_\vartheta \vartheta\right) \quad (10)$$

and the time derivative of (10) is approximated as

$$\frac{d}{dt} i_{ad} = \frac{\dot{\hat{\tau}}_L + J\ddot{\omega}_d + B\dot{\omega}_d + K_\vartheta \lambda_d \vartheta + K_\vartheta \lambda_d y_f}{K_\phi \phi_{fd}} - \frac{\left(\hat{\tau}_L + J\dot{\omega}_d + B\omega_d - K_\vartheta \vartheta\right)\dot{\phi}_{fd}}{K_\phi \phi_{fd}^2} \quad (11)$$

where λ_d is a gain which gives the speed of convergence of the second order filter (13), K_ϑ is a damping gain, the function ϑ is defined in (14) while y_f is the output of the second order filter (13b) and $\hat{\tau}_L$ denotes the estimated load torque and is obtained by means of the adaptation law

$$\dot{\hat{\tau}}_L = K_{\omega i} e_\omega \quad (12)$$

where $K_{\omega i}$ is the adaptation positive gain.

It is also required to obtain the approximation errors of the position and angular velocity by a second order filter of relative degree one, by means of a representation in the state space given by

$$\begin{bmatrix} \dot{x}_{1f} \\ \dot{x}_{2f} \end{bmatrix} = \begin{bmatrix} 0 & 1 \\ -\lambda_d^2 & -2\lambda_d \end{bmatrix} \begin{bmatrix} x_{1f} \\ x_{2f} \end{bmatrix} + \begin{bmatrix} 0 \\ \lambda_d^2 \end{bmatrix} e_\theta \quad (13a)$$

$$y_f = \begin{bmatrix} 0 & 1 \end{bmatrix} \begin{bmatrix} x_{1f} \\ x_{2f} \end{bmatrix} \quad (13b)$$

where y_f is the filtered angular velocity error, while e_θ is the angular position error, given by $e_\theta = \theta_d - \theta$ where θ is the angular position, θ_d is the desired angular position gotten from the integral of the desired angular velocity ω_d, and x_{1f} x_{2f} are the internal states of the filter. Furthermore, a function ϑ is defined as

$$\vartheta = x_{2f} + \lambda_d x_{1f} - \lambda_d e_\theta \quad (14)$$

The constants must satisfy the following: $K_{pa} > 0$, $K_{ia} > 0$, $K_{if} > 0$, $K_\vartheta > 0$, $\lambda_d > 0$ and

$$K_{pf} > \epsilon \frac{K_\phi^2}{4B} x_{2d}^2 \quad (15)$$

with $\epsilon > 0$.

The main control objective is to simultaneously achieve the global tracking of the rotor velocity and the field flux, and furthermore, assuring that all internal state variables are bounded.

C. Obtaining of the velocity by a second order filter

It is known that, the angular position θ is related to the angular velocity ω by

$$\frac{d}{dt}\theta = \omega(t) \quad (16)$$

To avoid using a derivative, according to (16), the velocity can be replaced through the use of a second order filter with relative degree 1, whose transfer function is

$$Y_f(s) = \frac{\lambda_d^2 s}{s^2 + 2\lambda_d s + \lambda_d^2} E_\theta(s) \quad (17)$$

where λ_d is a positive constant, $E_\theta\,(s)$ is the input variable, which is the error of the angular position in the domain of the complex variable s.

From the transfer function of the second-order filter, expressed in (17), some representations in the state space can be modeled. One of them is written in (13), with a function ϑ as it is shown in (14), which involves the internal states of the filter given in (13a) and the angular position error e_θ. The time derivative of ϑ is

$$\dot{\vartheta} = -\lambda_d \vartheta - \lambda_d e_\omega \quad (18)$$

with $e_\omega = \dot{e}_\theta$, according to that expressed in (16), is the error of the angular velocity.

D. Closed loop system

The state errors are defined as

$$\mathbf{e} = \mathbf{x}_d - \mathbf{x} \quad (19)$$

where $\mathbf{x}_d$ denote the desired states vector, in a particular way $\mathbf{e}^T = \begin{bmatrix} e_f & e_a & e_\omega \end{bmatrix} \in \mathbb{R}^3$, with

$$e_f = \phi_{fd} - \phi_f \qquad e_a = i_{ad} - i_a \qquad e_\omega = \omega_d - \omega \quad (20)$$

By taking into account the definition of the error states given in (19) and (20) and performing algebraic manipulation of (5) an equivalent equation of the close-loop is obtained as,

$$\boldsymbol{\mathcal{D}}\,\dot{\mathbf{e}} + \boldsymbol{\mathcal{R}}\,\mathbf{e} + \boldsymbol{\mathcal{C}}\left(\phi_f, i_{ad}, \omega_d\right)\,\mathbf{e} = \bar{\boldsymbol{\Psi}} \quad (21)$$

with $\bar{\boldsymbol{\Psi}} = \begin{bmatrix} \bar{\Psi}_f & \bar{\Psi}_a & \bar{\Psi}_\omega \end{bmatrix}^T \in \mathbb{R}^3$ and

$$\bar{\Psi}_f = -v_f + \dot{\phi}_{fd} + \frac{R_f}{L_f}\phi_{fd} - K_\phi \omega_d e_a + K_\phi i_{ad} e_\omega \tag{22a}$$

$$\bar{\Psi}_a = -v_a + L_a \frac{d}{dt} i_{ad} + R_a i_{ad} + K_\phi \phi_{fd} \omega_d \tag{22b}$$

$$\bar{\Psi}_\omega = \tau_L + J\dot{\omega}_d + B\omega_d - K_\phi i_{ad} \phi_{fd} \tag{22c}$$

The left side of (21) still have the matrices $\boldsymbol{\mathcal{D}}$ and $\boldsymbol{\mathcal{R}}$, which are positive definite and it has a matrix $\boldsymbol{\mathcal{C}}\left(\phi_f, i_{ad}, \omega_d\right) \in \mathbb{R}^{3x3}$ which is skew-symmetric, whose structure is

$$\boldsymbol{\mathcal{C}}\left(\phi_f, i_{ad}, \omega_d\right) = \begin{bmatrix} 0 & -K_\phi \omega_d & K_\phi i_{ad} \\ K_\phi \omega_d & 0 & K_\phi \, \phi_f \\ -K_\phi i_{ad} & -K_\phi \, \phi_f & 0 \end{bmatrix}. \tag{23}$$

From the equation (22a) with the supply voltages for the field windings proposed in (8), and simplifying, it results

$$\bar{\Psi}_f = -K_{pf}\, e_f - K_{if} \xi_f + K_\phi i_{ad} e_\omega \tag{24}$$

By choosing the desired currents for the armature windings as in (10), substituting in (22c) and simplifying, this gets to

$$\bar{\Psi}_\omega = K_\vartheta \vartheta + \left(\tau_L - \hat{\tau}_L\right) \tag{25}$$

On the other hand, by choosing the armature voltage proposed in (7) and substituting in (22b) it results

$$\bar{\Psi}_a = -K_{pa} e_a - K_{ia} \xi_a \tag{26}$$

In the expression for the armature voltage, given by (7), the time derivative of the desired armature current is required, which is obtained analytically by deriving respect to time (10), resulting as

$$\begin{aligned} \frac{d}{dt} i_{ad} = & \frac{\dot{\tau}_L + J\ddot{\omega}_d + B\dot{\omega}_d + K_\vartheta \lambda_d \vartheta + K_\vartheta \lambda_d \dot{e}_\theta}{K_\phi \phi_{fd}} \\ & - \frac{\left(\tau_L + J\dot{\omega}_d + B\omega_d - K_\vartheta \vartheta\right) \dot{\phi}_{fd}}{K_\phi \phi_{fd}^2} \end{aligned} \tag{27}$$

In (25) it can be seen the subtraction of the load torque from the estimated load torque, so that the load torque error is defined as

$$\tilde{\tau}_L = \tau_L - \hat{\tau}_L \tag{28}$$

where $\hat{\tau}_L$ is obtained by (12). The definition of error in (28) is according to adaptive control books. The time derivative of (28) considering assumption **A.5** is

$$\dot{\tilde{\tau}}_L = -K_{\omega i} e_\omega \tag{29}$$

In (27) the velocity error is required, but this is not available. Instead, in the implementation of the time derivative of the desired current, as it is presented in (11), the variable y_f is used, which is obtained through the representation of the second-order filter defined in (13b).

Let the states $\mathbf{e}$ and ϑ define a vector as $\bar{\mathbf{e}} = \begin{bmatrix} \mathbf{e} & \vartheta \end{bmatrix}^T \in \mathbb{R}^4$ and define the new state variables, introduced by the terms of the control laws (7) and (8), as $\boldsymbol{\xi} = \begin{bmatrix} \xi_f & \xi_a \end{bmatrix}^T \in \mathbb{R}^2$, where ξ_a and ξ_f are given in (9) with time derivatives given by

$$\dot{\xi}_f = e_f \qquad \dot{\xi}_a = e_a \tag{30}$$

So that, it is convenient to write the closed loop system formed by (18), (30) and what is obtained by substituting (24), (25) and (26) in (21). Thus, the closed loop system is

$$\bar{\boldsymbol{\mathcal{D}}}\dot{\bar{\mathbf{e}}} = -\bar{\boldsymbol{\mathcal{R}}}\,\bar{\mathbf{e}} - \bar{\boldsymbol{\mathcal{C}}}\left(\phi_f, \omega_d\right)\bar{\mathbf{e}} - \mathbf{I}_\xi^T \mathbf{K}_i \boldsymbol{\xi} + \mathbf{I}_{\tilde{\tau}} \tilde{\tau}_L \tag{31a}$$

$$\dot{\boldsymbol{\xi}} = \mathbf{I}_\xi \bar{\mathbf{e}} \tag{31b}$$

where the matrix $\bar{\boldsymbol{\mathcal{D}}} \in \mathbb{R}^{4x4}$ and $\mathbf{K}_i \in \mathbb{R}^{2x2}$ are structured as

$$\bar{\boldsymbol{\mathcal{D}}} = \begin{bmatrix} \boldsymbol{\mathcal{D}} & \mathbf{0}_{3x1} \\ \mathbf{0}_{1x3} & \frac{K_\vartheta}{\lambda_d} \end{bmatrix} \qquad \mathbf{K}_i = \begin{bmatrix} K_{if} & 0 \\ 0 & K_{ia} \end{bmatrix} \tag{32}$$

with the matrix $\boldsymbol{\mathcal{D}}$ defined in (6) and constants K_ϑ, λ_d, K_{if} and K_{ia} are strictly positive and the matrix $\bar{\boldsymbol{\mathcal{R}}} \in \mathbb{R}^{4x4}$, $\bar{\boldsymbol{\mathcal{C}}}\left(\phi_f, \omega_d\right) \in \mathbb{R}^{4x4}$, $\mathbf{I}_\xi \in \mathbb{R}^{2x4}$ and $\mathbf{I}_{\tilde{\tau}} \in \mathbb{R}^{4x1}$ whose structure are

$$\bar{\boldsymbol{\mathcal{R}}} = \begin{bmatrix} \boldsymbol{\mathcal{R}}_e & \mathbf{0}_{3x1} \\ \mathbf{0}_{1x3} & K_\vartheta \end{bmatrix} \tag{33a}$$

$$\bar{\boldsymbol{\mathcal{C}}}\left(\phi_f, \omega_d\right) = \begin{bmatrix} \boldsymbol{\mathcal{C}}_e\left(\phi_f, \omega_d\right) & -\mathbf{K}_\vartheta^T \\ \mathbf{K}_\vartheta & 0 \end{bmatrix} \tag{33b}$$

$$\mathbf{I}_\xi = \begin{bmatrix} \mathbf{I}_{2x2} & \mathbf{0}_{2x2} \end{bmatrix} \tag{33c}$$

$$\mathbf{I}_{\tilde{\tau}} = \begin{bmatrix} 0 & 0 & 1 & 0 \end{bmatrix}^T \tag{33d}$$

with $\mathbf{K}_\vartheta = \begin{bmatrix} 0 & 0 & K_\vartheta \end{bmatrix}$ and

$$\boldsymbol{\mathcal{R}}_e = \begin{bmatrix} \frac{R_f}{L_f} + K_{pf} & 0 & -K_\phi i_{ad} \\ 0 & R_a + K_{pa} & 0 \\ 0 & 0 & B \end{bmatrix} \tag{34a}$$

$$\boldsymbol{\mathcal{C}}_e\left(\phi_f, \omega_d\right) = \begin{bmatrix} 0 & -K_\phi \omega_d & 0 \\ K_\phi \omega_d & 0 & K_\phi \, \phi_f \\ 0 & -K_\phi \, \phi_f & 0 \end{bmatrix}. \tag{34b}$$

The vector of state variables for the complete closed loop system is defined as $\begin{bmatrix} \bar{\mathbf{e}}^T & \boldsymbol{\xi}^T \end{bmatrix}^T \in \mathbb{R}^6$, so that the origin is the unique equilibrium point of system defined by (31).

E. Main proposition

With all the background of this section, the following proposition is established:

Proposition 1. Consider the nonlinear mathematical model of a separately excited DC motor given by (5) in closed loop with the armature and field control voltage laws given by (7)-(14). Under assumptions **A.1**-**A.5**, positive gains $K_{pa} > 0$, $K_{ia} > 0$, $K_{if} > 0$, K_ϑ, $\lambda_d > 0$, and the condition given in (15), the closed loop system achieves global asymptotic velocity and field flux tracking, and all internal variables are bounded.

1) Proof: A quadratic function is now proposed in such a way that includes the states $\bar{\mathbf{e}}$, as well as $\boldsymbol{\xi}$ and $\tilde{\tau}_L$, as follows

$$\mathcal{H}_e = \frac{1}{2}\bar{\mathbf{e}}^T \bar{\boldsymbol{\mathcal{D}}}\bar{\mathbf{e}} + \frac{1}{2}\boldsymbol{\xi}^T \mathbf{K}_i \boldsymbol{\xi} + \frac{1}{2K_{\omega i}}\tilde{\tau}_L^2 \tag{35}$$

The quadratic function (35) satisfies

$$\Upsilon_{max}\Sigma \geq \mathcal{H}_e \geq \Upsilon_{min}\Sigma \tag{36}$$

with

$$\Upsilon_{max} = \frac{1}{2}\max\left(\lambda_{max}\left\{\bar{\boldsymbol{\mathcal{D}}}\right\}, \lambda_{max}\left\{\mathbf{K}_i\right\}, \frac{1}{K_{\omega i}}\right\} \tag{37a}$$

$$\Upsilon_{min} = \frac{1}{2}\min\left(\lambda_{min}\left\{\bar{\boldsymbol{\mathcal{D}}}\right\}, \lambda_{min}\left\{\mathbf{K}_i\right\}, \frac{1}{K_{\omega i}}\right\} \tag{37b}$$

$$\Sigma = \left(\|\mathbf{e}\|^2 + |\vartheta|^2 + |\xi_a|^2 + |\xi_f|^2 + |\tilde{\tau}_L|^2\right) \tag{37c}$$

and λ_{max} and λ_{min} denote the maximum and minimum eigenvalues, respectively, of the matrix between braces.

By deriving (35) with respect to time, substituting (31a), as well as (31b) and (29), considering that $\bar{\boldsymbol{\mathcal{C}}}\left(\phi_f, \omega_d\right)$ is skew-symmetric and simplifying, the following equation is obtained

$$\dot{\mathcal{H}}_e = -\bar{\mathbf{e}}^T \bar{\boldsymbol{\mathcal{R}}}_{sym}\bar{\mathbf{e}} \tag{38}$$

where the matrix $\bar{\mathcal{R}}_{sym}$ is the symmetric part of $\bar{\mathcal{R}}$, defined in (33a), must be positive definite to guarantee that the function given by (38) is negative semidefinite.

By applying the Sylvester's theorem to the $\bar{\mathcal{R}}_{sym}$ matrix, leads to conditions given in section III.B, so the proposed controller guarantees that the matrix $\bar{\mathcal{R}}_{sym}$ is positive definite. Satisfying these conditions, the function written in (35) is positive definite and decrescent, and (38) is a negative semidefinite function, therefore by using the Lyapunov theory (see e.g. Theorem 2.3 in [17, pag. 45]), it follows that the origin of the closed loop system (31) is a uniformly stable equilibrium; furthermore, because of the Lyapunov function (35) is a radially unbounded function, the signals $\mathbf{e}$, ϑ, $\boldsymbol{\xi}$ and $\tilde{\tau}_L$ will be uniformly bounded, for all initial conditions, by the following bounds

$$\|\mathbf{e}\| \leq \sqrt{2\lambda_{min}\left\{\mathcal{D}\right\}\mathcal{H}_e\left(0\right)} \tag{39a}$$

$$|\vartheta| \leq \sqrt{2\left(\lambda_d/K_\vartheta\right)\mathcal{H}_e\left(0\right)} \tag{39b}$$

$$|\xi_a| \leq \sqrt{\left(2/K_{ia}\right)\mathcal{H}_e\left(0\right)} \tag{39c}$$

$$|\xi_f| \leq \sqrt{\left(2/K_{if}\right)\mathcal{H}_e\left(0\right)} \tag{39d}$$

$$|\tilde{\tau}_L| \leq \sqrt{2K_{\omega i}\mathcal{H}_e\left(0\right)} \tag{39e}$$

where $\mathcal{H}_e(0)$ is (35) evaluated in initial time 0. Moreover, the norm of the vector $\bar{\mathbf{e}}$ complies with

$$\int_0^t \|\bar{\mathbf{e}}\|^2\, dt \leq \frac{\mathcal{H}_e\left(0\right)}{\lambda_{min}\left\{\bar{\mathcal{R}}\right\}} \tag{40}$$

The bounds given in (39) and (40) mean that $\mathbf{e} \in \mathcal{L}_\infty^3 \bigcap \mathcal{L}_2^3$, $\vartheta \in \mathcal{L}_\infty \bigcap \mathcal{L}_2$, $\int_0^t e_a dt \in \mathcal{L}_\infty$, $\int_0^t e_f dt \in \mathcal{L}_\infty$ and $\tilde{\tau}_L \in \mathcal{L}_\infty$. By considering this, from (21) it follows that $\dot{\mathbf{e}} \in \mathcal{L}_\infty^3$ and from (18) it follows that $\dot{\vartheta} \in \mathcal{L}_\infty$. and from (29) $\dot{\tau}_L \in \mathcal{L}_\infty$.

With all the aforementioned, sufficient conditions have been found to apply the Lemma 2.2 de [17, chap. 2, pag. 52]. That is, conditions for (35) and (38) are met, $\mathcal{H}_e > 0$ y $\dot{\mathcal{H}}_e \leq 0$. So, it results that $\bar{\mathbf{e}} \in \mathcal{L}_\infty^4 \bigcap \mathcal{L}_2^4$, $\boldsymbol{\xi} \in \mathcal{L}_\infty^2$ and that $\tilde{\tau}_L \in \mathcal{L}_\infty$. Also, according to (31a) it is fulfilled that $\dot{\bar{\mathbf{e}}} \in \mathcal{L}_\infty^4$. Because $\mathcal{H}_e$ is radially unbounded, it is concluded that the state errors $\bar{\mathbf{e}}$ globally asymptotically converges toward zero, i.e.,

$$\lim_{t\to\infty}\begin{bmatrix}\mathbf{e}\\ \vartheta\end{bmatrix} = 0\,.$$

This completes the proof of Proposition 1.

Remark 2. The condition (15) is subject to the desired armature current, which is calculated by (10). According to the structure of (10), assumption **A.4** guarantees that it does not have any singularity nor that it tends to infinity since ϕ_{fd} is strictly positive and upper and lower bounded. With assumption **A.3** it is guaranteed that the second and third members within the right side parenthesis of (10) are bounded, while with assumption **A.5**, the first term has to be bounded, and because $\vartheta \in \mathcal{L}_2$, it is concluded that the desired armature current is bounded. From (14) it is seen that as ϑ is bounded and under the assumption that the position error is bounded, this implies that the state x_{2f} is also bounded, and with assumptions **A.3**, **A.4**, **A.5** the time derivative of the desired armature current given in (27) is bounded, and because both the structure of the armature current as the integral terms are bounded, this implies that both control voltages are bounded.

Remark 3. The assumption **A.1** to **A.5** are not so restrictive. Assumption **A.1** is fulfilled under the availability of sensors for these variables; the assumption **A.2** is regularly complied with nameplate data and manufacturer specifications, with the use of measuring instruments as well as with experimental tests as suggested by many authors. Assumptions **A.3** and **A.5** arise from the stability analysis, and must be satisfied by the designer in order to ensure velocity tracking.

Remark 4. It should be mentioned that assumption **A.5** is made for simplicity in this proposal, and it has been widely used in the design of control strategies based on the passivity methodology for electrical machines when the estimation of the load torque by means of an adaptation law is used, as is the case of [18] and [19] for induction motors, or [20] for permanent magnet synchronous motors, or [11] and [16] for direct current motors. Likewise, there are also proposals for passivity where the load torque is assumed to be a known bounded function with first order derivatives.

Remark 5. As it can be seen in the equations that make up the controller (7)-(13), in the present proposal two independent reference signals are required: one for angular velocity; and the other for the field flux. These must meet the assumptions **A.3** and **A.4** and also must consider the nameplate data. Likewise, care must be taken to define the desired flux so that the machine is always operating in the linear region so that it does not become saturated.

IV. IMPLEMENTATION OF CONTROLLER.

The control algorithm given by equations (7), (8), (10), (11), the representation in the state space of the filter of second order of relative degree 1 (13), the function (14) and the conditions for the constants given in section III.B, were implemented in simulation and experimental form.

The machine considered in the simulation and experimental implementation is a DC Motor with field winding manufactured by Baldor-Reliance Model is D5505P, which can be seen in the Fig. 1. The nameplate data has the following rated values: armature voltage of 500 [V]; field voltage of $150/300$ [V]; field current $0.76/0.38$ [A]; angular velocity of $1750/2300$ [rpm] and a power of 5 [HP]. The configuration used is low voltage field excitation, i.e., parallel connection on the field colis.

Fig. 1. Direct Current Motor model D5505P.

As it can be seen, in the desired armature currents (10) as well as in its approximate derivative (11), it is required to have available the signal of the load torque and its derivative with respect to time. This is obtained by considering the adaptation law (12). Due to the unavailability of the angular velocity, in the experimental implementation the structure of the second order filter (13) is used. Then, to cope with this situation in the experimental implementation, the structure of the estimator of the load torque and its time derivative that were used are:

$$\hat{\tau}_L = K_{\omega i}\int y_f dt = K_{\omega i} x_{1f}, \quad \hat{\tau}_L(0) = 0 \tag{41a}$$

$$\dot{\hat{\tau}}_L = K_{\omega i} y_f = K_{\omega i} x_{2f} \tag{41b}$$

with $K_{\omega i} > 0$ and the variables x_{1f}, x_{2f} and y_f are obtained by (13). That is, the structure of the second order filter (13) is used to obtain the estimate of the load torque as well as its time derivative.

A. Measurement of parameters

The parameters of electrical nature, both in the field and armature, were obtained by means of a impedance measurement bridge, as well as in CC and CA experiments, as it is suggested in [21]. It is worth mentioning that tests were carried out at different voltage levels (both in CC and AC) and from there, the average values of resistance and inductance were obtained.

The value of the induced emf constant K_b can be obtained in an experimental way. This requires to couple the shaft of the machine of interest to another machine, so that the latter is used to rotate the DC motor at different speeds, as suggested in [21]. In this test, the DC electric machine was coupled with a three-phase permanent magnet synchronous motor (PMSM) manufactured by Baldor-Reliance model CSPM3611T with nameplate data: voltage $230/460$ [V]; velocity 1800 rpm, frequency to 60 Hz and power of 3 HP. Both motor were coupled with their shaft by means of a star coupling and the primary motor was manipulated at different speeds by means of an inverter YASKAWA V1000, model CIMR-VU2A0040FAA.

The voltage data are taken at the terminals of the armature winding at different speeds to make a graph (straight line on the origin) and the slope that results is the induced emf K_b constant. To do this, with the relationship in (1) and having a constant current in the field, called I_{f0}, it can be considered a constant flux as

$$\phi_{f0} = L_f I_{f0} \tag{42}$$

The induced emf constant K_b has a linear relation with the field flux [21, ch. 2], as

$$K_b = K_\phi \phi_f \ ; \tag{43}$$

and if K_b is available, as well as the field current I_{f0}, one has

$$K_\phi = \frac{K_b}{\phi_{f0}} = \frac{K_b}{L_f I_{f0}} \ . \tag{44}$$

During the test a constant supply voltage was provided in the field winding, so a constant current of $I_{f0} = 1.1406$ A was obtained. Due to this, the DC motor model given by (5) has a linear structure and the parameters of the mechanical nature are calculated from the angular velocity response graph which is obtained with the position signal as input to the representation in the state space of the second order filter given by (13). It should be mentioned that this graph was obtained by applying a voltage supply to the armature of 311 V and a few later seconds the voltage supply is shorted to the power reference. By applying linear control techniques (such as the final value theorem and the second order prototype equation) and considering the electrical parameters, the mechanical parameters are calculated.

The DC Motor parameters that were used for the simulation and experiments are: $R_a = 17.352\,\Omega$, $L_a = 36.274\times 10^{-3}$ H, $R_f = 158.96\,\Omega$, $L_f = 1.5477$ H, $B = 0.015170$ N m/rad/s, $J = 0.0012547$ Kg m^2 and $K_b = 3.007$ V s/rad. The constant K_ϕ is obtained by means of the expression given in (44) by considering the values of K_b and L_f and $I_{f0} = 1.1406$ A. (mentioned in Subsection IV.A).

The reference trajectory for the desired velocity was generated according to how it is developed in [22, sect. 2.3]. This velocity reference signal used in the simulation and experiment is given by

$$\omega_d = \begin{cases} 0, & 0 \le t \le t_0 \\ c_1(t-t_0)^2 + c_2(t-t_0)^3, & t_0 \le t \le t_1 \\ \omega_{max}, & t_1 \le t \le t_2 \\ c_1(t_3-t)^2 + c_2(t_3-t)^3, & t_2 \le t \le t_3 \\ 0, & t_3 < t \end{cases} \tag{45}$$

B. Simulation Results

For the simulation, the equations representing the mathematical model of the DC Motor (5) were used, these equations in conjunction with the controller equations, were implemented in the software Dynamic System Simulation (SIMULINK® version 7.5) for MATLAB®,[1] (version 7.10.0.499) of 32 bit (win34). Fixed step integration through Runge-Kutta method (ode4) was used with a sampling time of 0.00001 s. It should be mentioned that only basic SIMULINK® blocks were used.

The dynamic equations that describe the behavior of the DC motor are obtained neglecting some mechanicals characteristics. Due to this, in order to carry out the simulation experiment of the controller with the DC motor, a term that models dry or Coulomb friction is now included in the equation of the mechanical part of such machine; that is, the equation that is implemented in the structure of DC motor is

$$J\frac{d}{dt}\omega = K_\phi i_a \phi_f - B\omega - \tau_L - \mu_s \mathrm{sign}(\omega) \tag{46}$$

where $\mathrm{sign}(\cdot)$ is the sign function and μ_s is the static friction coefficient, so the last term on the right hand side of (46) is a torque due to dry friction on the machine shaft.

To start the simulation, it was considered a small constant load torque of $\tau_L = 0.15$ N-m and a field flux reference of

$$\phi_d = 0.1\sin(0.25t) + b_d \ \text{ Wb} \tag{47}$$

with $b_d = 0.8$. Also, the static friction coefficient of (46) is $\mu_s = 0.4$ while the time parameters of (45) were considered as $t_0 = 5$ s, $t_1 = 15$ s, $t_2 = 25$ s y $t_3 = 35$ s, while the maximum velocity was $\omega_{max} = 500$ rpm, therefore, a maximum acceleration of $\dot{\omega}_d = 75$ rpm/s is obtained in the time $t_{\dot{\omega}_{dmax}} = 10$ s.

The values of the constants K_{ia}, K_{pa}, K_{if}, ϵ, K_ϑ and $K_{\omega i}$ as well as the value of the constant λ_d used in simulation and in the real time experiment are: $K_{ia} = 100$, $K_{pa} = 0.05$, $K_{if} = 500$, $\epsilon = 0.15$, $K_\vartheta = 0.75$, $K_{\omega i} = 3$ and $\lambda_d = 75$.

In the Fig. 2, it can be observed the velocity response with the aforementioned load torque reference. In this Figure it can be seen that the actual velocity tracks the velocity given by (45) with $\omega_{max} = 500$ rpm. It can be seen that both graphs in

[1] SIMULINK and MATLAB are both trademarks of The Mathworks, Inc.

This article has been accepted for publication in a future issue of this journal, but has not been fully edited. Content may change prior to final publication. Citation information: DOI 10.1109/TIE.2021.3068683, IEEE Transactions on Industrial Electronics

the Fig. 2 (desired and actual velocity) are overlapping, except when the velocity reference begins to be different from zero to the 5 seconds. That is due to the effect to dry friction, the shaft has no movement until applied torque can move it. After this, in about 1.6 seconds later, the actual velocity tracks at desired velocity. A zoom box in the center of the Fig. 2 shows the response of both signals from seconds 5 to 7.

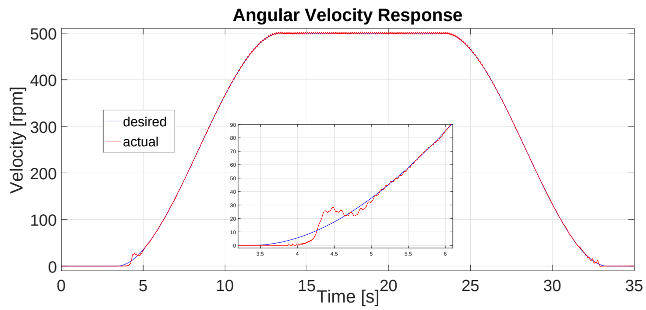

Fig. 2. Velocity response of the controller for the DC Motor (in simulation).

To explore the performance of the estimation of the load torque that is carried out by (41a) in conjunction with the controller, a simulation experiment is carried out with the same conditions mentioned at the beginning of this subsection, but considering that the load torque has different magnitudes at any given time of simulation as follow: from 0 to 10 seconds, of 0.1 N-m; from 10 to 20 seconds, of 5 N-m; from 20 to 30 seconds, of 1.5 N-m; and after 30 seconds, of 2.5 N-m.

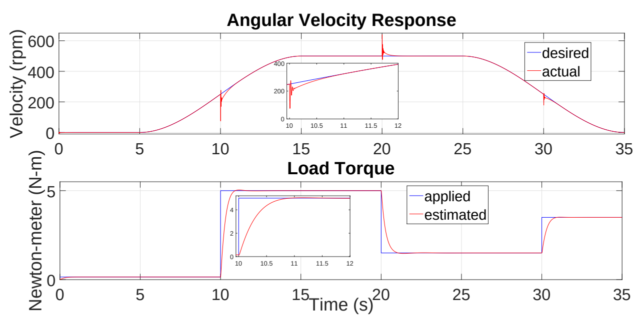

Fig. 3. Estimation of load torque used in non-linear DC motor controller (in simulation).

The upper graph of Fig. 3 shows the response of the angular velocity of the machine with the application of the load torque with different magnitudes, while the lower graph shows the estimation of the load torque. In both graphs there are zoom box from 10 to 12 seconds. In the zoom box of the velocity graph, it can be observed that when applying the load torque of 5 N-m at 10 seconds, after 0.1 s of simulation, the velocity response decreases to 74.77 rpm when the desired velocity is 250.6 (rpm) while in the zoom box for the load torque, it is observed that the estimation of the load torque has an overshoot of up to 5.15 N-m at 11.15 s. In all cases the velocity is recovered to the desired value and the estimated load torque achieves the actual torque, after a brief transient time.

Likewise, to analyze the electrical energy consumption of the machine (both in the field windings and in the armature) with different magnitudes of the field flux, a simulation experiment is carried out with the same conditions mentioned at the beginning of this subsection but at different bias b_d of the flux reference signal (47). In Fig. 4 the different total electrical powers developed by the DC motor are shown, having the same velocity response as shown in Fig. 2. It can be seen in the graphs that the greater the magnitude of the field flux there is a higher consumption of power or by performing a numerical integration of each of the powers it is verified that there is a lower electrical energy consumption when the magnitude of the field flux is lower. There is no information

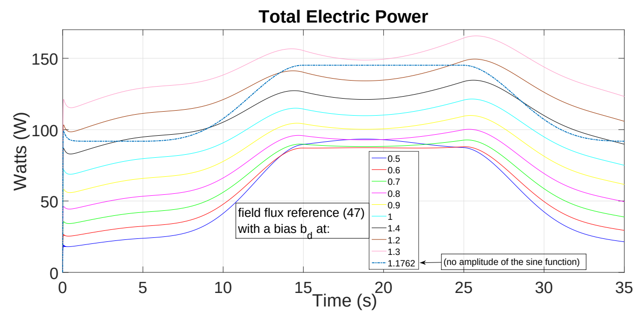

Fig. 4. Total electrical power (armature power plus field power) with different bias in the field flux reference signal (in simulation).

regarding nominal flux in the nameplate data. To obtain an approximate calculation of this, (1) is used considering the nominal current and the inductance obtained in the parameter measurements, this results as $\phi_{fn} = 1.1762$ Wb. In Fig. 4 the total power developed (blue color and dash-dot) of the machine is shown with a constant flux reference given by ϕ_{fn}, since this situation can be considered as the case of the motor with permanent magnet in the field. This study shows that for a same time variant reference of velocity the energy can be saved controlling simultaneously the field flux in a suitable way.

C. Experimental Results

The DC motor used in the experiments has the following instrumentation: the motor shaft has been coupled to a differential optical encoder of the Dynapar™ brand, model HS35R1024A10PS, hollow shaft of 16 mm of diameter, resolution of 1024 pulses per revolution(PPR), two channel quadrature (AB) and index (Z), Quadrature phasing $90° \pm 25°$ electrical, symmetry of PPR:$180° \pm 25°$ electrical. The electrical specifications are: input power of 5-26 VDC, 80 mA max; Output of open collector, 40 mA, frequency response at 125 kHz, noise immunity tested to ENG1326-1. In the Fig. 1 it can be seen the encoder on the right side of the motor.

The power supply for the armature and field windings were connected in series with the coil and with IGBTs (one before and another after each coil of the CD motor) to a direct current bus. For the case of the field, the DC bus is obtained by means of a simple rectification of a half bridge and filtering from a three-phase AC supply with a rms voltage of 220 V obtaining only 178 V.

The Fig. 5 shows the electronic circuit boards that are arranged to feed the armature and field windings in a variable and controlled way.

It is worth mentioning that for the physical experiments, the same SIMULINK® template that was generated for the

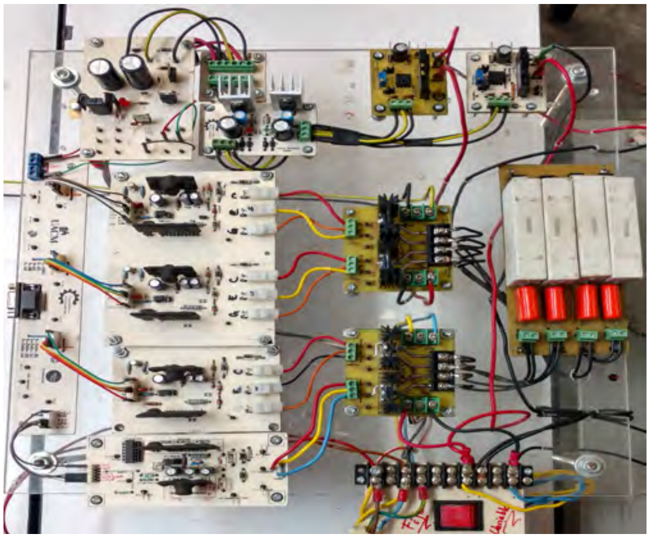

Fig. 5. Electronic circuit board.

simulation of the controller was used, only removing the blocks used to implement the mathematical model of the DC motor. The same fixed step integration was used, but now with a sampling time of 0.0001 s.

For processing the input and output signals in a PC, equipped with an Intel(R) Core(TM) i5-2500 CPU@3.30 GHz processor and 3.41 GB of RAM, a dSPACE 1103 controller card was used. The software of this card can directly provides the signal of the angular position in a SIMULINK® environment from the signals provided by the optical decoder.

The signals of both currents (field and armature) were obtained by means of Magneto-Resistive Current Sensors of the F.W. Bell, model NT-5 with primary nominal current I_{PN} of 5 A and overload at $10I_{PN}$, while output voltage at $\pm I_{PN}$ of ± 2.5 V as well as accuracy at I_{PN} and room temperature less $\pm 0.3\%$ and reaction time less $0.5\mu s$. The signals of the current sensors are obtained with a little noise, so a first-order filter was used by means of a basic block of SIMULINK® transfer function with a cutoff frequency of 500 rad/s with a unit gain.

The Fig. 6 shows a block diagram of the experimental setup, where the hardware structure mentioned in the last paragraphs is concentrated.

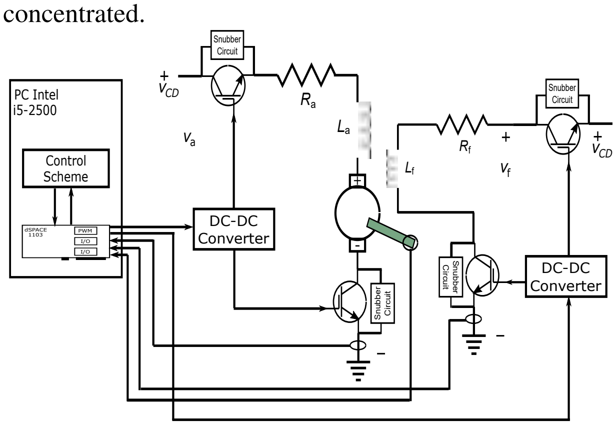

Fig. 6. Block diagram of the experimental setup

It is worth mentioning that the flux of the field was calculated according to equation (1), so the signal of the field current with a gain of L_f delivers the flux of the field, by this, it was considered that the field signal is available.

For the experiment, it was considered in the first instance that there is no load torque. It is worth mentioning that in fact, there is a load (small) coupled to the shaft by the fact of having the optical decoder directly coupled to the shaft. For the fact of not knowing how much load torque is present in the shaft, the torque estimator proposed by [19] given in equation (41a) is used.

For the carried out experiment, it was considered that the reference of the Field Flux were the same than the simulation given by (47) together its time derivative. Also, the same values of the gains given in section IV.B, as well as the same velocity reference signals given in (45), its first time derivative and its second time derivative were used.

In the Fig. 7, it can be observed the velocity response when there is a variant flux reference in the field given by (47). It can be seen that the actual velocity tracks the velocity reference. Also, in such a Fig. 7 it can be observed that at the moment of having a reference different from zero, the velocity response has a delay, close to 0.5 s due to the effect of dry friction, having a velocity tracking of 1.6 s later (red color graph). After this moment, in the remainder of the experiment, the angular velocity tracking is achieved. Also, in such a Fig. 7 it can be observed that at the moment of having a reference different from zero, the velocity response has a delay, close to 0.5 s due to the effect of the dry friction and to the low resolution of the optical encoder, which causes a velocity tracking of 1.6 s later (red color graph). After this moment, in the remainder of the experiment, the angular velocity tracking is achieved.

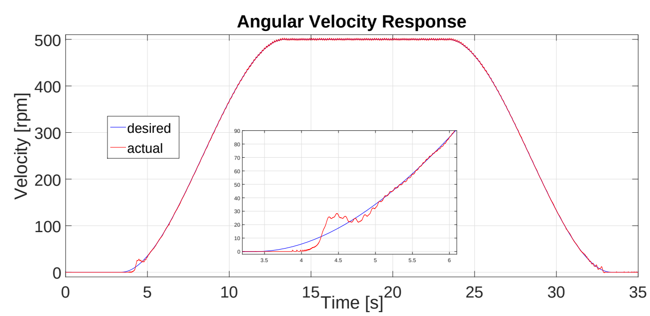

Fig. 7. Velocity response of the controller for the DC Motor.

In order to evaluate the difference between both velocities; in Fig. 8 it can be seen that the error has a peak with an amplitude of around 12 rpm close to zero velocity and at 500 rpm velocity reference, the error is around 3 rpm. Exactly in zero velocity reference the error is zero. Precisely when the velocity reference is very close to zero is when it presents a bit more speed error (when the reference starts from zero and when it returns to zero).

In the Fig. 9 the desired (blue) and actual (red) field flux are shown. It can be seen from the Figure that the desired flux has the form due to the equation (47) and the actual flux follows this reference. It should be mentioned that the field flux is not measured directly, but it is obtained by using (1) with the current signal provided by the magnetoresistive

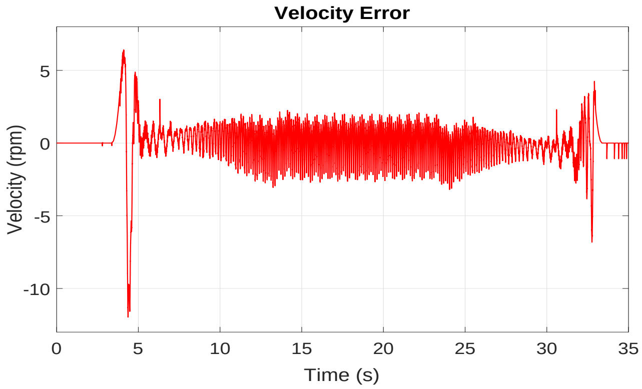

Fig. 8. Angular velocity error.

sensor. The voltage supplied by the sensor is noisy, which when is multiplied by the inductance of the field windings, the calculated flux has a noise amplification of approximately 50 percent more.

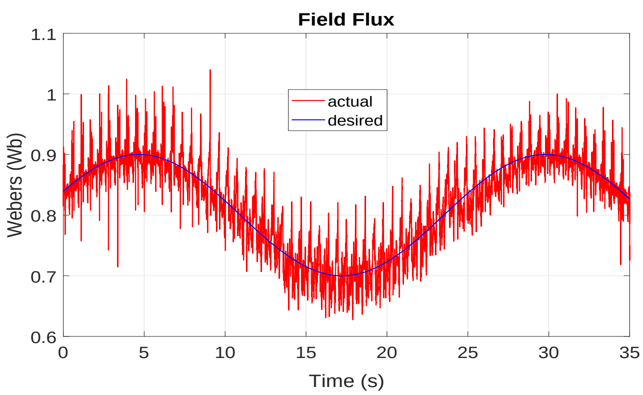

Fig. 9. Flux in the winding of the field.

To obtain the required field flux, the Fig. 10 shows the control voltage required in the field windings. It can be observed how the voltage that is required to obtain the field flow is varying.

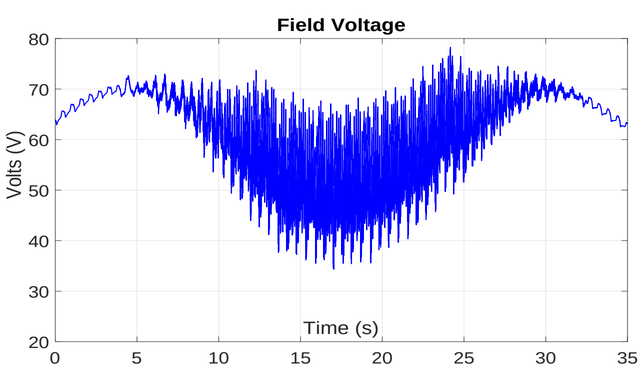

Fig. 10. Control voltage in windings of the field.

In Fig. 11, it can be seen the desired (blue) and the actual (red) current of the armature windings. As it can be observed in the Fig. 11 the current is within the allowed limits of the machine. The computed desired current is more noise than the actual current. As it can be seen in the equation of the desired currents (10), there is a term that involves the function ϑ given by (14), which is constructed from the position error; even when this signal is required to track the speed, the actual current is less noisy than the desired current.

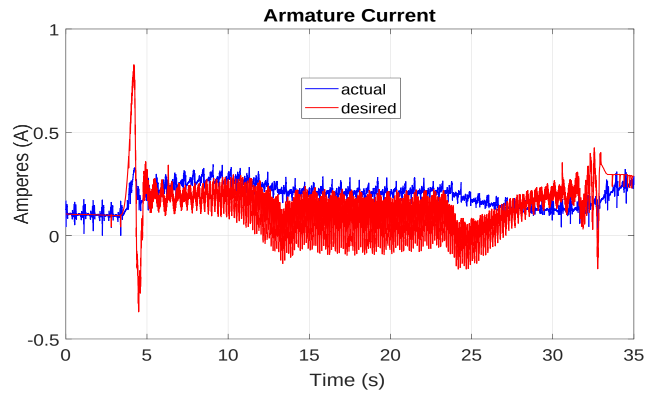

Fig. 11. Currents in the armature windings.

Due to the structure of the desired current, the required voltage in the armature windings is also variant in an small magnitude, as it can be seen in the Fig. 12. The armature voltage is within the allowed limits of the machine.

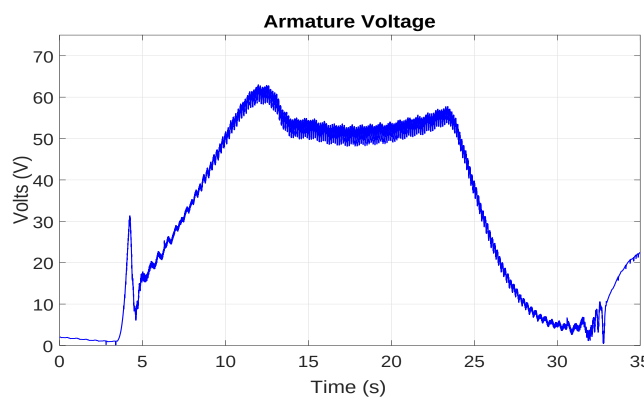

Fig. 12. Control voltage in windings of the armature.

V. Conclusion

In this paper, it is reported a new proposal of simultaneous control scheme of angular velocity and field flux tracking of the nonlinear DC motor with separately field excitation, without velocity measurement, where it is considered that the available signals for feedback are the angular position, as variable of mechanical origin, together with the currents of both windings, as variables of electrical origin. In this scheme, unlike those reported for the classical DC motor, there is the freedom to incorporate two signals, simultaneously, as references: one for the variable of mechanical nature, the desired angular velocity and the other for the variable of magnetic nature in the field, the desired field flux. Moreover, integral terms of current error are incorporated in the control voltages, as is emperically done in industrial applications. The controller equations are physically implementable, so both time variant reference signals are tracked, which is a difference and advantage over the established classical schemes. It is worth mentioning, which is formally demonstrated, via Lyapunov's theory, that the proposed controller ensures global asymptotic tracking of angular velocity, armature current and field flux; and in addition, all state variables are bounded.

Likewise, it was verified by means of computer simulation in SIMULINK® the aforementioned theoretical proposal. In the same sense, in spite of do not having the exact knowledge of the parameters, nor considering in the controller design the switched power supplies in the windings of the armature and field and not having the availability of the signal of the load torque, the present design was implemented in physical form (real-time experiments), keeping the tracking of the references of angular velocity and field flux.

The future works of the machine with this structure are various. One is to consider the mathematical model of switched sources in the controller design, i.e., to take into account the nonlinear structure of the motor, as well as the structure of the power supplies (of both windings), considering as input reference, both the angular velocity and the flux of the field to perform a control strategy such as the one proposed in the present work. Another is performing a sensorless control strategy for the structure of the non-linear model of the DC motor. One more is using estimation of parameters to have a more exact knowledge of the motor parameters. In the matter of hardware, improving the switching sources to be able to have both, positive and negative references.

Acknowledgment

This work is supported by Universidad Autónoma de la Ciudad de México (UACM) and partially supported by CONACYT Project 134534, and TecNM Projects.

References

[1] S.-K. Sul, *Control of electric machine drive systems*, vol. 88. John Wiley & Sons, 2011.

[2] B. C. Kuo and F. Golnaraghi, *Automatic control systems*, vol. 9. Prentice-Hall Englewood Cliffs, NJ, 1995.

[3] M. R. Reis, F. S. Silva, W. R. Araújo, W. P. Calixto, D. S. Araújo, I. N. Mendes, and R. M. Rose, "Speed control for direct current motor using optimization tuning for pid controller," in *Environment and Electrical Engineering (EEEIC), 2016 IEEE 16th International Conference on*, pp. 1–4. IEEE, 2016.

[4] R. K. Achanta and V. K. Pamula, "Dc motor speed control using pid controller tuned by jaya optimization algorithm," in *2017 IEEE International Conference on Power, Control, Signals and Instrumentation Engineering (ICPCSI)*, pp. 983–987. IEEE, 2017.

[5] A. T. Mohamed, M. F. Mahmoud, L. A. Said, and A. G. Radwan, "Design of fopid controller for a dc motor using approximation techniques," in *2019 Novel Intelligent and Leading Emerging Sciences Conference (NILES)*, vol. 1, pp. 142–145. IEEE, 2019.

[6] G. E. Marmidis and A. T. Alexandridis, "A passivity-based pi control design for dc-drives," in *Control and Automation, 2009. MED'09. 17th Mediterranean Conference on*, pp. 1511–1516. IEEE, 2009.

[7] J. Linares-Flores and H. Sira-Ramirez, "Dc motor velocity control through a dc-to-dc power converter," in *Decision and Control, 2004. CDC. 43rd IEEE Conference on*, vol. 5, pp. 5297–5302. IEEE, 2004.

[8] J. Yang, H. Wu, L. Hu, and S. Li, "Robust predictive speed regulation of converter-driven dc motors via a discrete-time reduced-order gpio," *IEEE Transactions on Industrial Electronics*, vol. 66, no. 10, pp. 7893–7903, 2018.

[9] A. T. Alexandridis and G. C. Konstantopoulos, "Modified pi speed controllers for series-excited dc motors fed by dc/dc boost converters," *Control Engineering Practice*, vol. 23, pp. 14–21, 2014.

[10] L. An, T. Cheng, and D. D.-C. Lu, "Single-stage boost-integrated full-bridge converter with simultaneous mppt, wide dc motor speed range, and current ripple reduction," *IEEE Transactions on Industrial Electronics*, vol. 66, no. 9, pp. 6968–6978, 2018.

[11] C. Guerrero, V. Santibañez, Y. Araiza-Olvera, E. Ibarra-Figueroa, and B. Pérez-Pérez, "Control of velocity of dc motors by classical and passivity methods measuring only position: Theory and experimental comparison," *IEEE Latin America Transactions*, vol. 18, no. 05, pp. 962–970, 2020.

[12] H. Chu, B. Gao, W. Gu, and H. Chen, "Low-speed control for permanent-magnet dc torque motor using observer-based nonlinear triple-step controller," *IEEE Transactions on Industrial Electronics*, vol. 64, no. 4, pp. 3286–3296, 2016.

[13] I. Dimeas, I. Petras, and C. Psychalinos, "New analog implementation technique for fractional-order controller: a dc motor control," *AEU-International Journal of Electronics and Communications*, vol. 78, pp. 192–200, 2017.

[14] M. Bodson and J. Chiasson, "Differential-geometric methods for control of electric motors," *International Journal of Robust and Nonlinear Control*, vol. 8, no. 11, pp. 923–954, 1998.

[15] Z. Z. Liu, F. L. Luo, and M. H. Rashid, "Speed nonlinear control of dc motor drive with field weakening," in *Industry Applications Conference, 2001. Thirty-Sixth IAS Annual Meeting. Conference Record of the 2001 IEEE*, vol. 1, pp. 541–547. IEEE, 2001.

[16] D. U. Campos-Delgado, E. Palacios, and D. R. Espinoza-Trejo, "Passivity based control of nonlinear dc motors configurations and sensorless applications," in *Industrial Electronics, 2007. ISIE 2007. IEEE International Symposium on*, pp. 3379–3384. IEEE, 2007.

[17] R. Kelly, V. Santibáñez, and A. Loría, *Control of robot manipulators in joint space*, 1st ed. Springer Science & Business Media, 2006.

[18] R. Ortega, P. J. Nicklasson, and G. Espinosa-Pérez, "On speed control of induction motors," *Automatica*, vol. 32, no. 3, pp. 455–460, 1996.

[19] H. Mujica, G. Espinosa-Pérez, and J. Mareno, "Seguimiento de velocidad y flujo magnético con alto desempeño en motores de inducción," *XVI Congreso Latinoamericano de Control Automático, CLCA 2014*, 2014.

[20] A. Achour, B. Mendil, S. Bacha, and I. Munteanu, "Passivity-based current controller design for a permanent-magnet synchronous motor," *ISA transactions*, vol. 48, no. 3, pp. 336–346, 2009.

[21] R. Krishnan, *Electric Motor Drives. Modeling, Analysis and Control*. Prentice Hall, Inc., 2001.

[22] J. Chiasson, *Modeling and High-Performance Control of Electric Machines*. John wiley & Sons, Inc., 2005.

Cuauhtémoc Guerrero (BS'93-MS'00-PhD'06) was born in Copala, Guerrero, México. He received the BS. degree in Electrical Engineering from Instituto Tecnológico de Saltillo, México and his MS. and PhD. degree in Electrical Engineering from the Universidad Nacional Autónoma de México in 1993, 2000 and 2006 respectively.

He is currently a professor at the Universidad Autónoma de la Ciudad de México. His research interests are control of electrical machines and electrical drives, nonlinear systems control, and passivity based control.

Víctor Santibañez (BS'77-MS'84-PhD'97) was born in San Pedro de las Colonias, Coahuila, México. He received the BS. and MS. degree in Electronics Engineering from Instituto Tecnológico de la Laguna and his PhD. degree from CICESE Research Center, Ensenada, México in 1977, 1984 and 1997 respectively.

From 1977 to 1981 he worked in the respective Industrial Electronics Departments of the iron and steel industry at Altos Hornos de Mexico and Metalúrgica Mexicana Peñoles. From 1989 to 1990 he was with the Instituto de Automática Industrial (CSIC) in Madrid Spain. He is the author/coauthor of many peer reviewed journal and international conference papers. He has served as reviewer of a number of prestigious scientific journals. He has coauthored two books on robot control: Control of Robot Manipulators (in Spanish, Prentice Hall, 2003) and Control of Robot Manipulators in Joint Space (Springer, 2005). He is currently Professor with Instituto Tecnológico de la Laguna. His research interests are robot control, nonlinear systems control, fuzzy control and adaptive control.